Electronic Supporting Information (ESI)

for

Tandem Indium Oxide-Boron Nitride Catalysts for Oxidative Dehydrogenation of Propane

Lei Cao,[a] Peng Xu,[b] Guohui Zhong,[a] Yifan Wu,[a] Sheng Wen,[c] Rongliang Shang,[a] Yixiao Liu,[a] Pengcheng Dai,[b,*] Jin Xie[a,*]

[a]*School of Physical Science and Technology & Shanghai Key Laboratory of High-resolution Electron Microscopy, ShanghaiTech University, Shanghai, 201210, China. E-mail:* xiejin@shanghaitech.edu.cn

[b]*College of New Energy, State Key Laboratory of Heavy Oil Processing, China University of Petroleum (East China), Qingdao 266580, China. E-mail:* dpcapple@upc.edu.cn

[c]*College of Engineering and Applied Sciences, Nanjing University, Nanjing, 210093, China.*

Table of contents

1. Experimental Procedures

1.1 Fabrication of xIn_2O_3-BN catalyst

In a typical deposition process, In_2O_3 atomic clusters were formed at 150 °C, Cyclopentadienyl indium (InCp) used as the indium precursor, was heated to 90 °C. Water vapor and plasma oxygen were introduced into the ALD chamber to remove the ligand. A typical deposition cycle included: InCp injection (0.15 s) - exposure (30 s) - argon purging (90 s) - water injection (0.15 s) + O_2 plasma (20 s) - argon purging (90 s). h-BN with different indium oxide loading was obtained by controlling the ALD cycles, resulting in material named *x*cIn_2O_3-BN (where *x* indicates the number of ALD cycles).

1.2 General procedure for oxidation dehydrogenation of propane

The as-prepared *x*cIn_2O_3-BN catalyst (100 mg) was placed in the middle of the quartz tube (I.D. = 9 mm) and supported by quartz wools. A K-type thermocouple was inserted into the center of the catalyst bed to monitor the operating temperature. The reactant gas mixture, consisting of nitrogen, propane, and oxygen in a 6:1:1 ratio, had a total flow rate of 24 mL min^{-1}, controlled by three mass flow controllers. The outlet gas was analyzed by an on-line gas chromatograph (FULI INSTRUMENTS, GC9790II) equipped with a HP-PLOT Al_2O_3 column (30 m × 0.53 mm × 15 μm), a Porapak Q packed column (2 m × 3 mm) and 5A molecular sieve

column (2 m × 4 mm). A flame ionization detector (FID) was used for detecting of CH_4, C_2H_6, C_2H_4, C_3H_8 and C_3H_6, etc., while CO, CO_2 and CH_4 were detected using a thermal conductivity detector (TCD). Every *x*cIn_2O_3-BN catalyst was activated at a propane conversion of ~ 20% for 15 min, after which the reactor was cooled to 460 °C for catalytic evaluation. The reaction temperature was varied in the range of 460 - 560 °C with a ramp of 2 °C min^{-1} (reactant gas: N_2-C_3H_8-O_2 = 6-1-1, total flow rate = 24 mL min^{-1}, WHSV = 14400 L kg_{cat}^{-1} h^{-1}). Such a low reaction gas concentration can avoid the formation of excessive oxygenate, while creating a low water vapor concentration environment. The long-term stability test was performed at the reaction temperature where propane conversion was ~ 15%.

1.3 Equations

The propane conversion, product selectivity, yield and carbon balance were calculated as follows:

$$\text{Propane conversion} = \frac{\text{C mol of } \left(C_3H_{8,IN} - C_3H_{8,OUT}\right)}{\text{C mol of } C_3H_{8,IN}} \times 100\%$$

$$\text{Product selectivity} = \frac{\text{C mol of specific product}}{\text{C mol of } \left(C_3H_{8,IN} - C_3H_{8,OUT}\right)} \times 100\%$$

$$\text{Product yield} = (\text{Propane conversion} \times \text{Product selectivity}) \times 100\%$$

$$\text{Carbon Balance} = \frac{\text{C mol of (products+}C_3H_{8,OUT})}{\text{C mol of } C_3H_{8,IN}} \times 100\%$$

where C mol refers to the number of carbon moles in the products, inlet and outlet of the propane.

1.4 Catalysts Characterization

Transmission electron microscopy (TEM), including high-resolution transmission electron microscopy (HRTEM) was obtained using a JEM F200 Electron Microscope operated at 200 kV. Thermal gravimetric (TG) analysis was performed on a thermal analyzer (Netzsch TG/209F3). Powder X-ray diffraction (PXRD) patterns were collected on a Bruker D8 X-ray diffractometer with Cu Kα radiation at room temperature. The Fourier transform infrared (FT-IR) spectra of the samples were recorded on a Bruker 4700 FT-IR spectrometer (Bruker Optics Inc., Ettlingen, Germany). X-ray photoelectron spectroscopy (XPS) spectra were collected on an ESCALAB 250Xi X-ray photoelectron spectrometer. Inductively coupled plasma optical emission spectrometer was performed on an Agilent ICPOES 720. Nitrogen physisorption isotherms were recorded at 77 K using a Quantachrome Autosorb-iQ nitrogen volumetric adsorption instrument. Before measurement, the catalysts were degassed at 120 °C for 8 h. The scanning transmission electron microscopy (STEM), energy-dispersive X-ray spectroscopy (EDS), and electron energy loss spectroscopy (EELS) elemental mapping and spectra were collected on a JEOL Grand ARM-300F, operate at 300 kV with a Gatan Oneview camera and a K2 summit direct electron counting detector. Non-local density

functional theory (NLDFT) calculations were performed to obtain the pore size distribution based on the measured N_2 adsorption isotherms.

2. Supplementary Figures and Tables

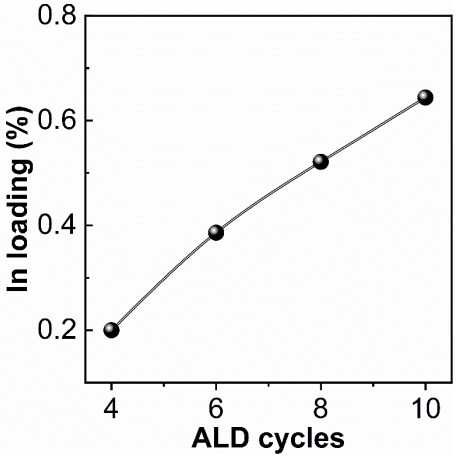

Fig. S1 Indium loadings in *x*cIn_2O_3-BN with different ALD deposited cycles determined by ICP-OES.

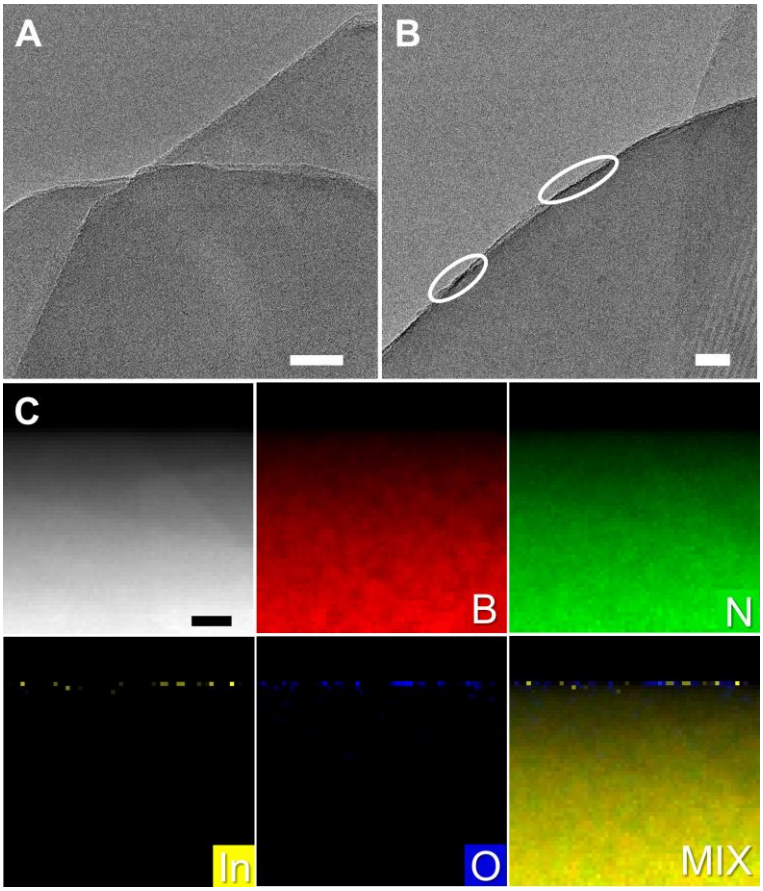

Fig. S2 TEM images of fresh BN (A) and 8cIn_2O_3-BN (B) catalysts. Scale bars: 20 nm. (C) STEM image and corresponding EELS elemental mapping of fresh 4cIn_2O_3-BN catalyst, high-lighting the distribution of key elements. Scale bars: 10 nm.

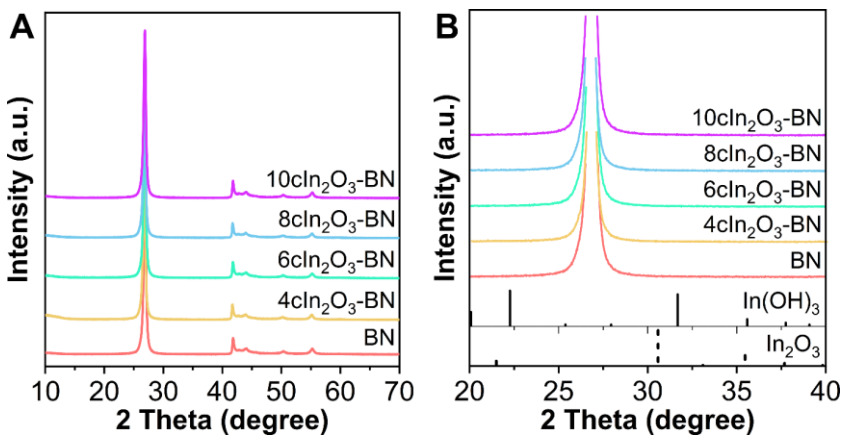

Fig. S3 XRD patterns of fresh *x*cIn$_2$O$_3$-BN composite catalysts.

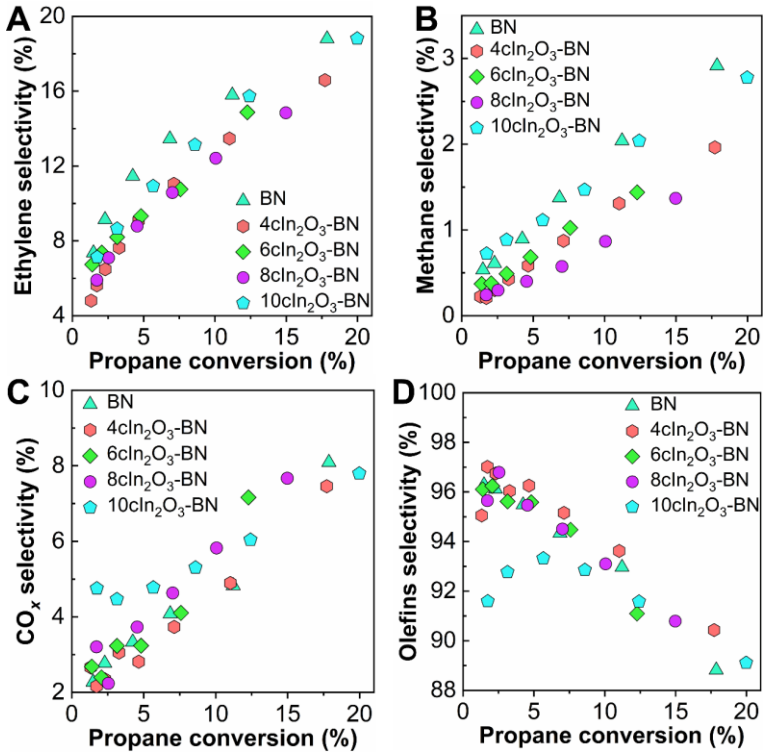

Fig. S4 Olefins selectivity and ethylene selectivity as a function of propane conversion over BN and *x*cIn$_2$O$_3$-BN catalysts.

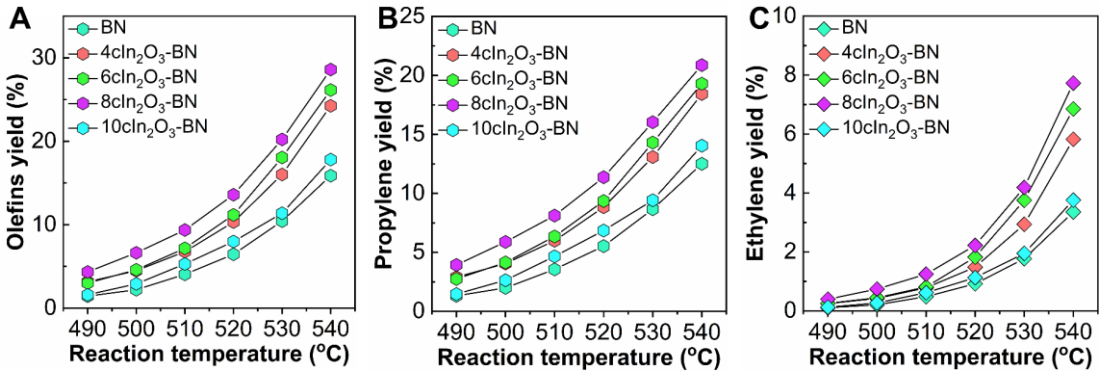

Fig. S5 Olefins, propylene, and ethylene yield as a function of reaction temperature over pristine BN and *x*cIn$_2$O$_3$-BN catalysts.

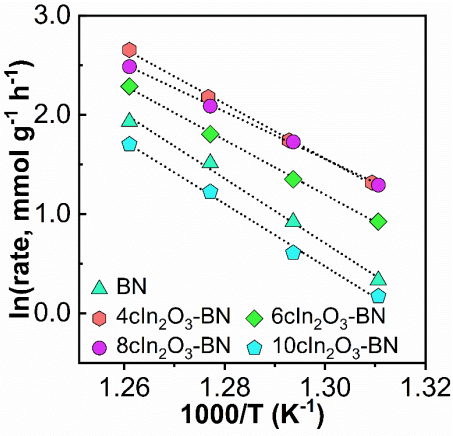

Fig. S6 Reaction rate as a function of reaction temperature over pristine BN and *x*cIn$_2$O$_3$-BN catalysts.

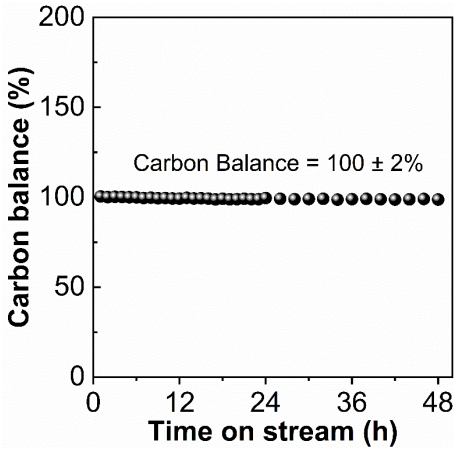

Fig. S7 Carbon balance during the long-term stability test.

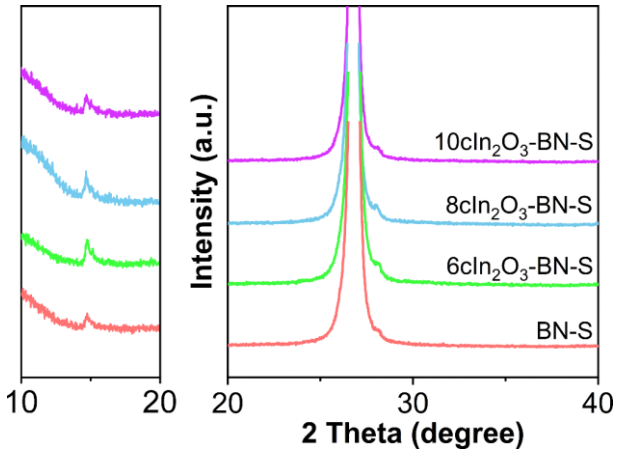

Fig. S8 XRD patterns of spent BN and *x*cIn$_2$O$_3$-BN composite catalysts.

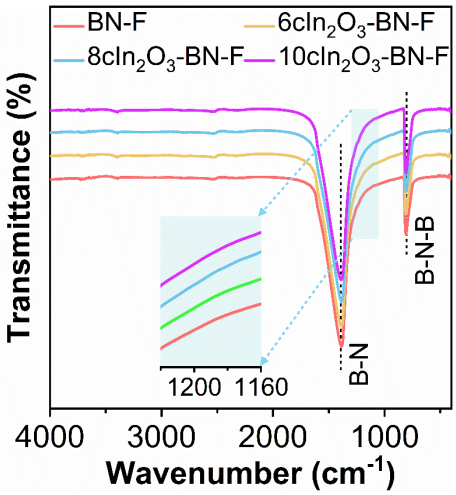

Fig. S9 FT-IR spectra of fresh *x*cIn$_2$O$_3$-BN (*x*cIn$_2$O$_3$-BN-F) and BN (BN-F) catalysts.

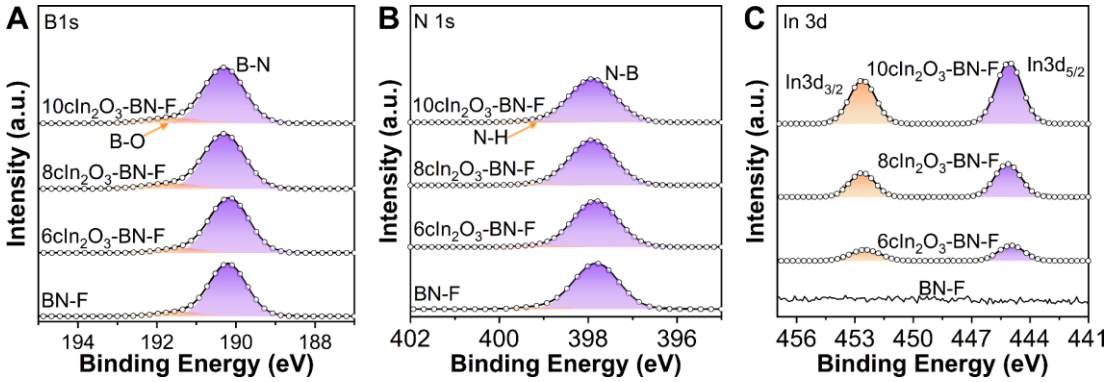

Fig. S10 XPS spectra of B 1s (a), N 1s (b), and In 3d (c) from fresh *x*cIn$_2$O$_3$-BN catalysts.

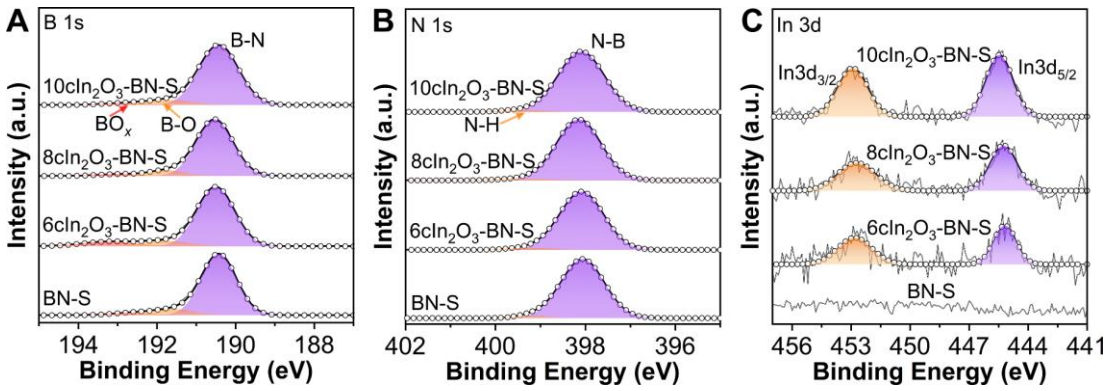

Fig. S11 XPS spectra of B 1s (a), N 1s (b), and In 3d (c) from spent *x*cIn$_2$O$_3$-BN catalysts.

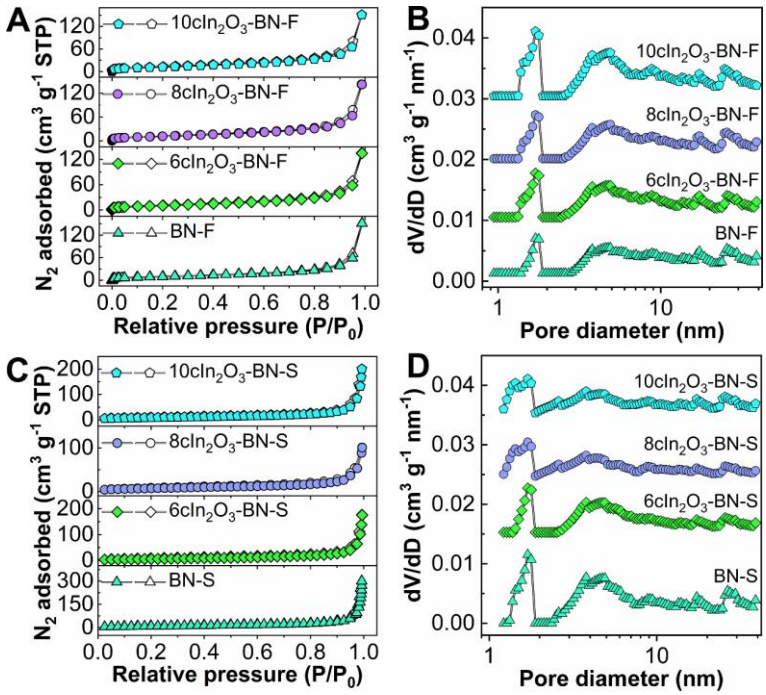

Fig. S12 Nitrogen adsorption-desorption isotherm and corresponding pore distribution of fresh (a-b) and spent (c-d) *x*cIn$_2$O$_3$-BN catalysts.

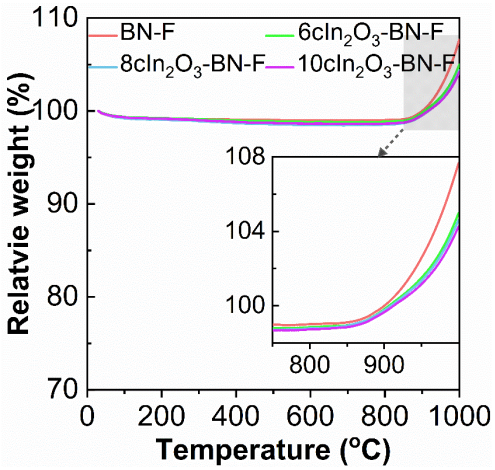

Fig. S13 TGA curves of fresh *x*cIn$_2$O$_3$-BN catalysts.

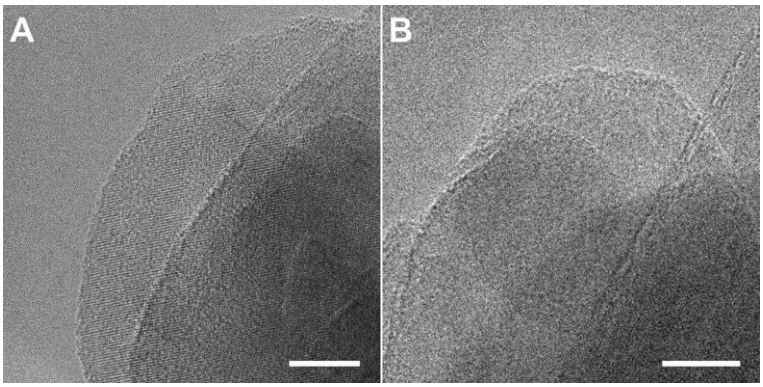

Fig. S14 TEM images of spent BN catalysts, scale bars: 10 nm.

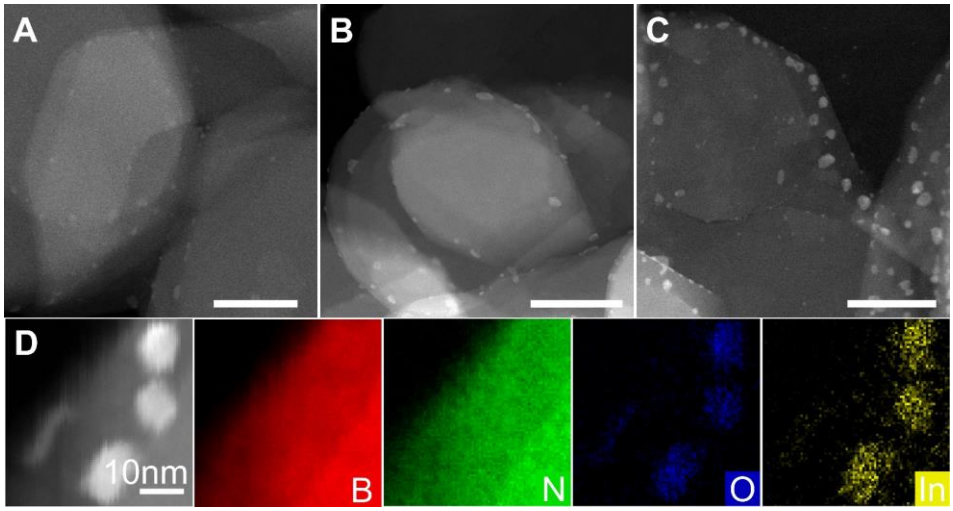

Fig. S15 STEM images of spent 6cIn_2O_3-BN (a), 8cIn_2O_3-BN (b), and 10cIn_2O_3-BN (c) catalysts. scale bars: 100 nm. STEM images of 10cIn_2O_3-BN and corresponding EELS elemental mappings (d).

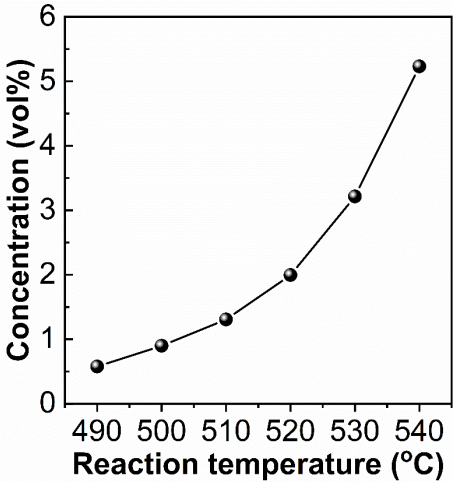

Fig. S16 Water vapor concentration as a function of reaction temperature.

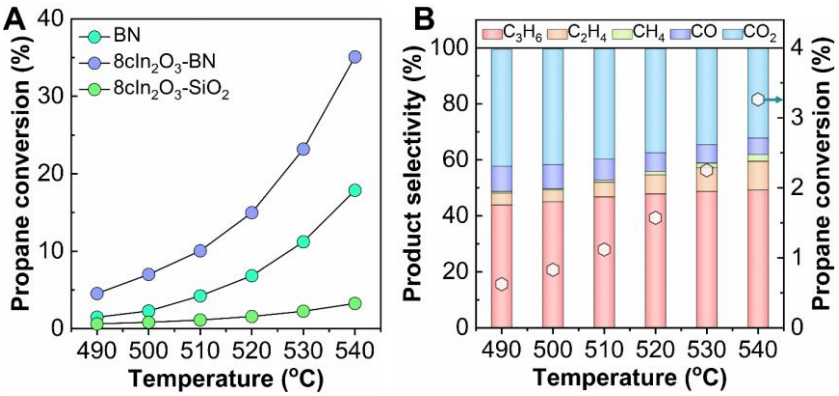

Fig. S17 (a) Comparison of catalytic performance of BN, 8cIn$_2$O$_3$-BN, and 8cIn$_2$O$_3$-SiO$_2$. (b) Product selectivity and propane conversion over 8cIn$_2$O$_3$-SiO$_2$ catalyst as a function of reaction temperature.

Table S1. Comparison of apparent activation energy (*E*a) between pristine BN and

various *x*cIn$_2$O3-BN catalysts.

Catalysts	***E*a (kJ mol^{-1})**	***R*^{2}**
p-BN	271.1±1.6	0.995
4cIn$_2$O$_3$-BN	229.5±5.3	0.998
6cIn$_2$O$_3$-BN	228.6±6.6	0.998
8cIn$_2$O$_3$-BN	197.8±3.2	0.999
10cIn$_2$O$_3$-BN	261.9±1.3	0.997

Table S2. The amount of BO_x species of fresh and spent BN and $8cIn_2O_3$-BN catalysts.

Catalysts	**BN**	**$8cIn_2O_3$-BN**
Fresh	7.9%	2.9%
Spent	3.9%	3.1%

Table S3. Brunauer-Emmett-Teller (BET) surface area and pore volumes of fresh and spent BN and *x*cIn_2O_3-BN catalysts.

Catalysts	**BET surface area ($m^2\ g^{-1}$)**	**Pore volume ($cm^3\ g^{-1}$)**
Fresh BN	35.7	0.12
Spent BN	52.8	0.18
Fresh 6cIn_2O_3-BN	38.0	0.12
Spent 6cIn_2O_3-BN	23.5	0.09
Fresh 8cIn_2O_3-BN	42.2	0.14
Spent 8cIn_2O_3-BN	34.9	0.11
Fresh 10cIn_2O_3-BN	45.7	0.12
Spent 10cIn_2O_3-BN	27.3	0.07